Journal of Medicinal Chemistry

ARTICLE

pubs.acs.org/jmc

Design and Synthesis of Imidazopyridine Analogues as Inhibitors of Phosphoinositide 3-Kinase Signaling and Angiogenesis

Okseon Kim,[†,§] Yujeong Jeong,[†,§] Hyunseung Lee,[‡,§] Sun-Sun Hong,[*,‡] and Sungwoo Hong[*,†]

[†]Department of Chemistry, Korea Advanced Institute of Science and Technology (KAIST), Daejeon 305-701, Korea

[‡]Department of Biomedical Sciences, College of Medicine, Inha University, Incheon, 400-712, Korea

ABSTRACT: Phosphatidylinositol 3-kinase α (PI3Kα) is an important regulator of intracellular signaling pathways, controlling remarkably diverse arrays of physiological processes. Because the PI3K pathway is frequently up-regulated in human cancers, the inhibition of PI3Kα can be a promising approach to cancer therapy. In this study, we have designed and synthesized a new series of imidazo[1,2-*a*]pyridine derivatives as PI3Kα inhibitors through the fragment-growing strategy. By varying groups at the 3- and 6-positions of imidazo[1,2-*a*]pyridines, we studied the structure−activity relationships (SAR) profiles and identified a series of potent PI3Kα inhibitors. Representative derivatives showed good activity in cellular proliferation and apoptosis assays. Moreover, these inhibitors exhibited noteworthy antiangiogenic activity.

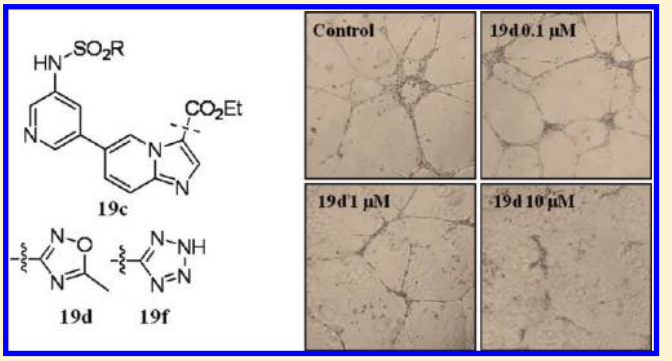

1. INTRODUCTION

Angiogenesis is a physiological process involving the growth of new blood vessels from preexisting vessels, which is crucial for tumor growth, invasion, and metastasis. Tumor angiogenesis can be triggered by extracellular signals such as vascular endothelial growth factor (VEGF) when the tumor reaches 1−2 mm in diameter. Solid tumors contain hypoxic regions that have considerably lower oxygen tension than the normal tissues. The transcription factor hypoxia-inducible factor 1 (HIF-1) is a major regulator of tumor cell adaptation to hypoxic stress and activates transcription of the promoter of VEGF, a key factor of tumor angiogenesis. Many antibodies have been developed to neutralize the action of the VEGF and have successfully inhibit the formation of new blood vessels that are required for solid tumor growth.[1]

Recent studies have shown that the PI3K/Akt pathway plays critical roles in angiogenesis and in the expression of HIF-1α and VEGF.[2,3] Our research was stimulated by the fact that inhibition of the PI3K/Akt pathway could lead to potent antiangiogenic activity against human cancer cells. Phosphoinositide 3-kinases (PI3Ks) are lipid kinases that catalyze phosphorylation of the 3-hydroxyl position of PIP2 (phosphatidylinositol 4,5-bisphosphate) to form PIP3 (phosphatidylinositol 3,4,5-trisphosphate). In response to growth factors, PI3K can be activated by receptor protein tyrosine kinases (RTKs) and by nonreceptor protein tyrosine kinases. The resulting second messenger PIP3 involves multiple physiological processes, including cell growth, differentiation, survival, and motility.[4] Among different subtypes of PI3Ks, the *PIK3CA* gene encoding PI3K p110α is frequently mutated and overexpressed in a large portion of human cancers such as ovarian, breast, gastric, and hepatocellular carcinomas.[5] These observations strongly suggest that the PI3K pathway including PTEN inactivation mediates angiogenesis and tumor growth by regulating VEGF and HIF-1 expression.[6,7] Therefore, the inhibition of the PI3K/Akt pathway (PI3K/Akt, HIF-1α, VEGF) has been considered to be a powerful approach for the treatment of cancer. We describe here our studies on the design and synthesis of imidazopyridine-based PI3Kα inhibitors through the fragment-based growing strategy and demonstrate the therapeutic evaluation of these compounds in terms of antiangiogenic and antiproliferative effect on cancer cells.

2. RESULTS AND DISCUSSION

2.1. Design of New PI3K Inhibitors. The recent availability of the three-dimensional structure of therapeutic targets has enhanced opportunities for the rapid development of active compounds utilizing structure-based design. Fragment-growing strategy has been efficiently used in many structure-based drug design programs.[8] A starting building block can be grown into a novel ligand with high affinity by adding interacting moieties to a starting scaffold. As proteins occur in families characterized by conserved binding motifs, they can be addressed by a privileged skeleton which binds to the common motif of a protein family. Some heterocyclic fragments mimicking the purine portion of adenosine-5′-triphosphate (ATP) can bind to the hinge region of

Received: December 14, 2010
Published: March 09, 2011

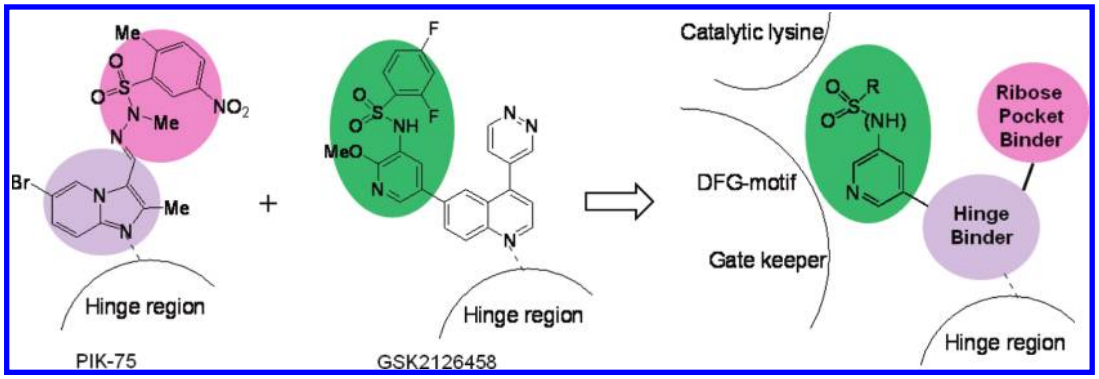

Figure 1. Design of new scaffolds as PI3K inhibitors and opportunities for modification in the schematic active site of PI3K.

the kinase via hydrogen bonds with the backbone and represent starting points for a fragment-growing approach.

With a goal to develop a new structural class of potent PI3K inhibitors, we initiated a pharmacophore-directed design. To assess the back pocket (DFG-motif, gate keeper, and catalytic lysine), we took advantage of the information in the literature in search of well-established modulators of this pocket.[9,10] Among various moieties which can interact in the back pocket, the pyridyl sulfonamide moieties have demonstrated a high degree of inhibitor efficiency and several PI3Kα inhibitors had been built from these groups.[9] On the basis of an inspection of this class of inhibitors in the public domain and our previously gained insights into the binding mode of this moiety,[9f] the pyridyl sulfonamide moiety was selected as a putative building block. Thus, our design strategy prioritized the incorporation of this pharmacophore into the appropriate hinge binder to generate novel hybrid molecules with potent activity. Furthermore, we planned to extend the structures by attaching additional groups of suitable shape, size, and polarity to fill the ribose binding site. For example, the alignment of PIK-75[11] compound and GSK2126458[9e] reveals that the shaded portions of each compound fills different regions within the binding pocket, implying that joining these components into a single molecule might impart enhanced potency by exploiting extended interactions (Figure 1).

2.2. Imidazopyridine Moiety as Hinge Binder. Recently, patent disclosure has described a number of new PI3K inhibitors using the 2-chloro or methoxy pyridyl sulfonamides.[9g] While fixing a *N*-(pyridin-3-yl)benzenesulfonamide moiety, our initial round of analogues was focused around incorporation of a variety of heterocycles to identify the most suitable hinge region binder. We analyzed a number of known kinase inhibitors as well as heterocycles that would be anticipated to have the propensity to bind to the hinge region. The preparation of the target compounds is described in Scheme 1. The synthesis commenced with treatment of the commercially available pyridyl bromide (**1**) with benzene sulfonyl chloride in CH_2Cl_2, followed by borylation with bis(pinacolato)diboron to afford the corresponding boronic ester **2**. Various heteroaryl groups were then attached to the pyridyl sulfonyl moiety using a palladium-catalyzed cross-coupling to furnish the target compounds **3** as shown in Scheme 1.

The resulting compounds in which various heterocycles were grown from the pyridyl sulfonamide moiety to reach into a hinge region of the PI3K, were tested over PI3Kα at 10 μM concentration in a high-throughput binding assay (KINOMEscan, Ambit Biosciences). Several compounds were discovered as hits

Scheme 1[a]

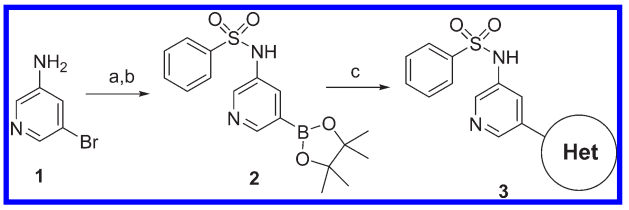

[a] Reagents and conditions: (a) $PhSO_2Cl$, pyridine, CH_2Cl_2, rt; (b) bis(pinacolato)diboron, $PdCl_2(dppf)\cdot CH_2Cl_2$, KOAc, 1,4-dioxane, 100 °C; (c) aryl bromide, $PdCl_2(dppf)\cdot CH_2Cl_2$, K_2CO_3, 1,4-dioxane/water = 3:1, 100 °C.

[POC (percent of control) values < 60] as shown in Table 1. Of particular significance is the observation that a profound effect on potency was achieved by the combination of the pyridyl sulfonamide moiety with imidazopyridine scaffold (POC = 6). Considering tolerance within the PI3Kα active site and low molecular weight of 350, compound **3e** is expected to serve as a good scaffold from which much more potent inhibitors can be derivatized. The imidazopyridine moiety has also been shown or proposed to be the hinge-region binding group in other kinase inhibitors.[11,14] For these reasons, **3e** was selected for further optimization to embark upon in-depth structural modification.

To obtain structural insight into the inhibitory mechanisms of the identified inhibitors of PI3Kα, their binding modes in the ATP-binding site were investigated in a comparative fashion. From the overall structural features derived from docking simulations, the inhibitory activity of **3e** is likely to stem from the multiple hydrogen bonds and hydrophobic interactions. Thus, examination of the hinge-region/imidazopyridine interaction in the PI3Kα homology model[12,13] showed that the imidazopyridine of **3e** maintains the hydrogen-bonding pattern in the hinge region (Val851). The pyridyl group is anchored by a hydrogen bond to the Y836, and the sulfonamide binds to the catalytic lysine (Lys802), as shown in Figure 2. These three hydrogen bonds seem to play a role of anchor for binding of **3e**. The benzene ring forms hydrophobic interactions with several hydrophobic residues in the active site. Building upon the success observed with the imidazopyridine scaffold, an investigation of the effect of the appendage at the C3 position was planned to probe the ribose binding pocket. The imidazopyridine scaffold can be easily equipped with functional groups at the C3 position

by standard synthetic chemistry, allowing substitutions for rapid exploration of the SAR profile.

2.3. Exploration of C3 Appendage. Finding lead-level inhibitors, we next focused our design attempts on the filling of a neighboring hydrophobic pocket occupied by the ribose moiety of ATP. On the basis of the modeling considerations regarding the space and environmental polarity of this space, variable sizes at the C3 position ranging from cyano group to various substituted aromatic ring system were introduced. First, compounds containing small groups (e.g., carbonyl, ester, and cyano groups) at C3 were prepared as initial controls to estimate experimentally the gain in binding free enthalpy resulting from penetration of the ribose pocket. The general synthetic route for the preparation of imidazopyridine derivatives is shown in Scheme 2. In general, the C3 position of the imidazopyridine was functionalized prior to performing a Suzuki coupling at the C6 position. The starting material 5-bromopyridin-2-amine (**4**) was treated with 1,1-dimethoxy-*N*,*N*-dimethylmethanamine in refluxing methanol, followed by cyclization of the resulting enamine **5** with the suitable alkyl halides, afforded either nitrile or methyl ketone. The nitrile functional group of **6** was converted to oxadiazole **7** by a two-step sequence: condensation with (1) hydroxylamine hydrate, followed by (2) acetic anhydride. The pyridyl sulfonamide group at the C6 position was then installed by Suzuki coupling, followed by sulfonylation. Tetrazole analogue **9** was obtained by direct conversion of the nitrile to tetrazole upon treatment with NaN_3 using $CdCl_2$ as Lewis acid. Treatment of the methyl ketone of **10** with 1,1-dimethoxy-*N*,*N*-dimethylmethanamine, and then hydrazine hydrate, provided pyrazole analogue **11**.

To install heteroaromatic rings at the C3 position, the C3 position was first iodinated. Thus, condensation of **4** with chloroacetaldehyde, followed by iodination at the C3 position using *N*-iodosuccinimide in acetonitrile at room temperature afforded the corresponding 3-iodo-imidazopyridine **12**. Various aryl groups were then attached at the C3 position using a palladium-catalyzed cross-coupling to furnish compounds **13**. Finally, target compounds **14** were prepared by the two-step sequence shown in Scheme 2. Thus, Suzuki coupling of 6-bromoimidazo[1,2-*a*]pyridine **13** with corresponding boronic esters, followed by sulfonylation with appropriate sulfonyl chloride, afforded the desired products **14**. In some cases, sulfonylation was performed prior to Suzuki coupling due to the nature of substituents at the C3 position of imidazopyridine analogues. To further increase structural diversity at C6, various sulfonamide groups (R′: Me, Ph, substituted benzene, heterocycles, and revered sulfonamide) were connected to the C6 through Suzuki coupling.

To build the ester group at the C3 position, 5-bromopyridin-2-amine (**4**) was treated with ethyl 2-chloro-3-oxopropanoate potassium salt to afford ester **15**, followed by Suzuki coupling with corresponding boronic acids to give compound **16**. In the

Table 1. Array of Various Heterocycles and Early Hits

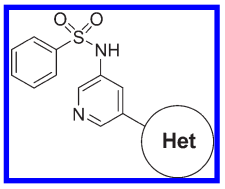

Cpd	Het	POC[a]
3a		52
3b		33
3c	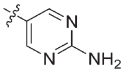	52
3d	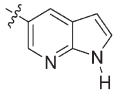	44
3e	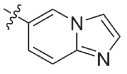	6
3f	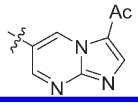	41

[a] Compounds with POC < 60 against PI3Kα at 10 μM concentration are shown. Lower numbers of POC (percent of control) indicate stronger hits. Values show an average of duplicate measurements.

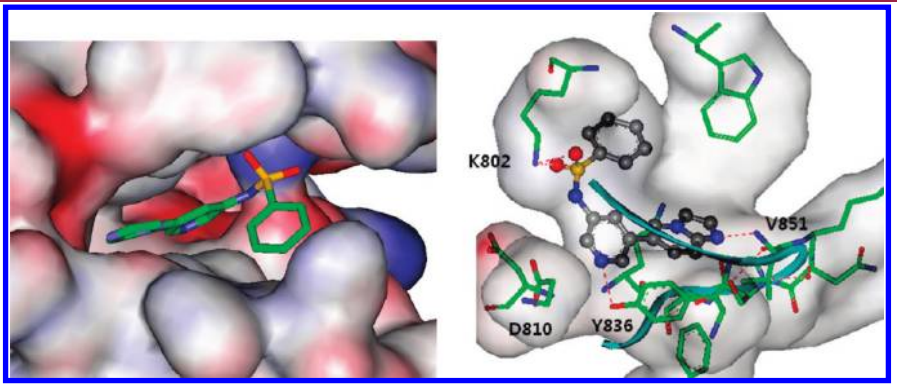

Figure 2. Putative binding mode of **3e** with the PI3Kα homology model, based on PI3Kγ crystal structures. In this model, the nitrogen of imidazole moiety forms a key hinge region hydrogen bond with the backbone of Val851, and the sulfonamide binds to the catalytic lysine (Lys802). Selected residues (D810 and Y836) are shown for possible interaction with pyridyl sulfonamide subunit.

Scheme 2. Synthetic Route of Imidazopyridine Derivatives[a]

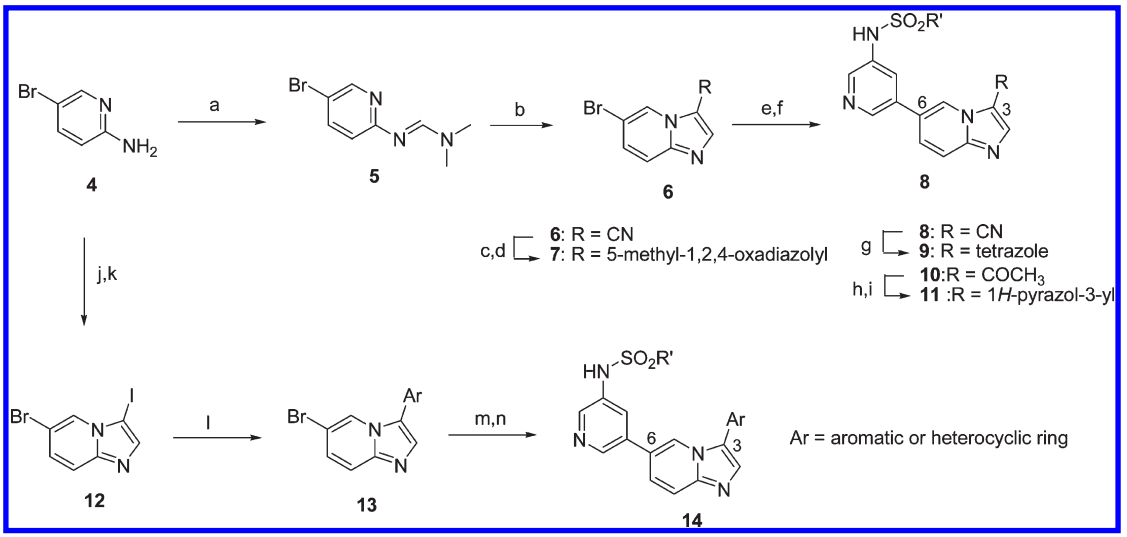

[a] Reagents and conditions: (a) $Me_2NCH(OMe)_2$, MeOH, 70 °C; (b) RCH_2Br, *i*-PrOH, $NaHCO_3$, 100 °C; (c) $HONH_2.HCl$, Et_3N, EtOH, rt; (d) Ac_2O, 1,4-dioxane, 100 °C; (e) arylboronic ester, $PdCl_2(dppf)\cdot CH_2Cl_2$, K_2CO_3, 1,4-dioxane/water = 3:1, 100 °C; (f) benzenesulfonyl chloride, pyridine, DCM, rt; (g) NaN_3, $CdCl_2$, DMF, 100 °C; (h) $Me_2NCH(OMe)_2$, reflux; (i) $H_2NNH_2.H_2O$, EtOH, reflux; (j) $ClCH_2CHO$, $NaHCO_3$, *i*-PrOH, 100 °C; (k) NIS, CH_3CN, rt; (l) arylboronic acid, $PdCl_2(dppf)\cdot CH_2Cl_2$, K_2CO_3, 1,4-dioxane/water = 3:1, 80 °C; (m) arylboronic ester, $PdCl_2(dppf)\cdot CH_2Cl_2$, K_2CO_3, 1,4-dioxane/water = 3:1, 100 °C; (n) RSO_2Cl, pyridine, CH_2Cl_2, rt.

Scheme 3[a]

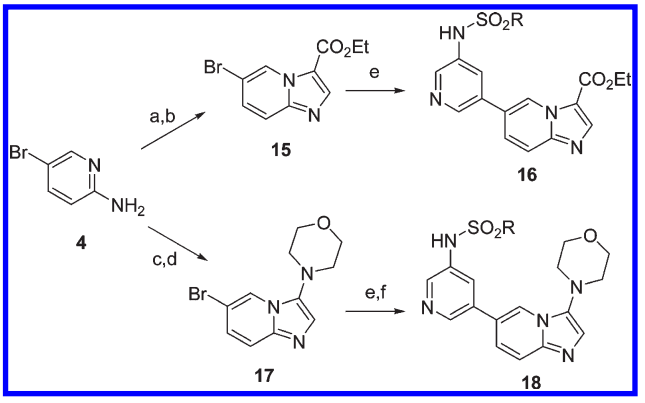

[a] Reagents and conditions: (a) HCO_2Et, $ClCH_2CO_2Et$, KO*t*Bu, DIPE, 0 °C to RT; (b) conc H_2SO_4, EtOH, 90 °C; (c) benzotriazole, morpholine, glyoxal, EtOH, rt; (d) 1,2-dichloroethane, 80 °C then KOH, rt; (e) arylboronic ester, K_2CO_3, $PdCl_2(dppf)\cdot CH_2Cl_2$, 1,4-dioxane/water = 3:1, 100 °C; (f) $PhSO_2Cl$, pyridine, CH_2Cl_2, rt.

case of morpholine analogues, benzotriazole-mediated cyclization gave compound **17** with a morpholyl substituent (Scheme 3). The introduction of the morpholine moiety was intended to improve the water solubility of these derivatives, which is required for planned cell-based assays.

Inhibitory activity against PI3Kα was determined by measuring the POC at 10 μM compound concentration as a primary screen. Compounds with POC < 10 were progressed into full IC_{50} value determination and, depending on their activity, tested against cancer cells to determine the cellular activity. The first series of compounds which contain oxygen and nitrogen capable of functioning as a hydrogen-bond acceptor (e.g., methyl ketone, ester, and cyano groups) at the C3 position showed potent inhibition activity over PI3Kα as shown in Table 2. Notably, ester-containing analogue **19c** (Figure 3) is an exceptionally potent PI3Kα inhibitor with an IC_{50} of 0.8 nM. However, **19c** is somewhat unstable in an aqueous phosphate buffer (pH 6.7) solution; about 8% of **19c** decomposed at 40 °C over 48 h. Because instability is probably due to the hydrolysis of the ester linkage of **19c**, we investigated ester surrogates. Thus, efforts focused on a search for ester bioisosteres such as oxadiazole or thiadiazole that could maintain potent PI3Kα inhibition while improving stability. Conversion of the ester group in **19c** to the bioisosteric 1,2,4-oxadiazole group gave compound **19d**, which exhibited almost equipotent PI3Kα activity with an IC_{50} of 2 nM and was completely stable under the same conditions. This successful replacement prompted further investigation through synthesis of a series of structurally related heterocycles. Some heterocycles were well tolerated, and in tetrazole ring **19f**, a modest increase in activity was observed (IC_{50} = 0.8 nM). Similarly, pyridyl derivatives **19j** and **19k** resulted in compounds which were generally of equivalent enzyme potency and possessed good activity in a cellular proliferation assay. In contrast, the pyrazole group gave derivative **19e**, which featured a 100-fold reduction in potency (IC_{50} = 213 nM) compared with oxadiazole analogue **19d**. The morpholine moiety was employed to enhance the physicochemical properties, but incorporation of a morpholine group at the C3 position slightly decreased potency. Introduction of a benzene ring at the C3 position also decreased the PI3Kα inhibitory activity, implying the importance of the heteroatoms at this region for PI3K inhibition. Intriguingly, the cyano group at the 3-position on the benzene ring of **19h** was effective in producing PI3Kα inhibitory activity (IC_{50} = 12 nM). In the next design cycle, we examined the SAR of the sulfonamide groups, and the highest PI3Kα potency was obtained with 2,4-diF substituted phenyl groups (IC_{50} of **19p** = 0.6 nM). Reversal of the sulfonamide connectivity led to **19l**, which showed increased solubility but decreased enzyme activity.

dx.doi.org/10.1021/jm101582z |*J. Med. Chem.* 2011, 54, 2455–2466

Table 2. Structure−Activity Relationship with R^1 and R^2 Groups

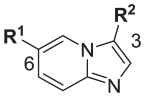

19

Compd	R^1	R^2	PI3Kα IC_{50} (nM)
3e	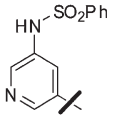	H	360
19a		COMe	2
19b		CN	11
19c		CO_2Et	0.8
19d		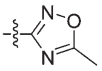	2
19e		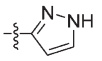	213
19f		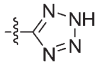	0.8
19g		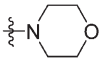	36
19h		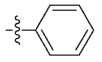	720
19i		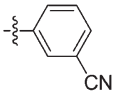	12
19j		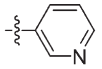	7
19k		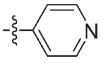	4
19l	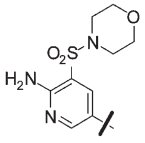	CN	47
19m		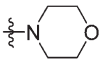	480
19n		CN	10
19o	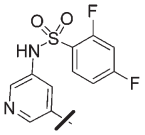	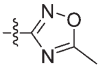	2
19p		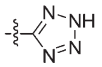	0.6
19q	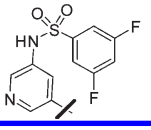	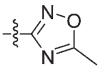	81

[a] IC_{50} values against PI3Kα determined using PI3-Kinase Glo kit (Promega Inc.). Data are mean values for two independent experiments performed in duplicate with standard error of <20%.

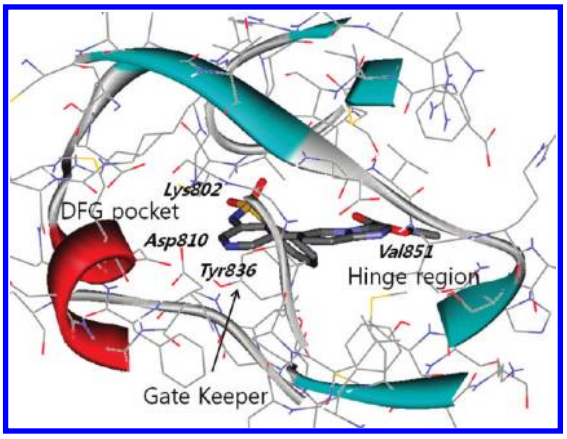

Figure 3. Docking of **19c** in PI3Kα homology model based on PI3Kγ crystal structures.

Table 3. KINOMEscan Profile of Compound 19d[a]

kinase	POC[b]	K_d (nM)	kinase	POC[b]	K_d (nM)
CDK11	0.1	88	PIK3C2B	0	ND
CDK7	1.4	ND	PIK3CA	0	1.2
CSNK1G2	0.55	ND	PIK3CB	0.015	25
mTOR	0	39	PIK3CG	0	ND

[a] Panel of 98 kinases were tested at 10 μM in a high-throughput binding assay (Ambit Bioscience). [b] Kinases with POC < 5 at 10 μM concentration are shown. Lower numbers of POC (percent of control) indicate stronger hits. Values show an average of duplicate measurements.

Table 4. Inhibition of Cancer Cell Proliferation for Selected Compounds

	Growth IC_{50} (μM)		
compd	T47D	SK-BR3	MCF7
19a	3.2	11	11
19b	2.9	1.4	37
19c	0.6	1.5	7.8
19d	1.1	1.2	1.5
19j	7.5	15	>50
19k	1.6	7.3	11
19o	0.8	0.7	7.2
19q	8.3	9.2	>50

To obtain the detailed picture of this series, **19d** was tested at 10 μM concentration in a high-throughput binding assay (KINOMEscan, Ambit Biosciences) across a panel of 98 human kinases. Eight kinases displayed tight binding to **19d**, and dissociation constants were determined for CDK11, mTOR, PI3Kα, and PI3Kβ as shown in Table 3. Similar to the other reported PI3K inhibitors, **19d** is a pan-PI3K/mTOR inhibitor and showed modest specificity profiles against other protein kinases.

2.4. Antiproliferation Activity. Given the impressive enzyme activity profile, several potent compounds from this series were further tested for cellular proliferation activity against cancer cell lines. To measure the inhibitory effect of compounds on cell

dx.doi.org/10.1021/jm101582z |J. Med. Chem. 2011, 54, 2455–2466

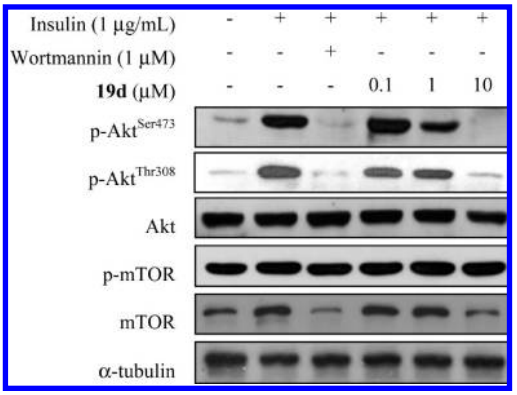

Figure 4. Inhibition of cellular PI3K signaling in T47D. T47D cells were treated with various concentration of **19d** for 30 min, and the PI3K pathway was activated by treatment of 1 μg/mL insulin for 2 h. Compound **19d** decreased the phosphorylation of Akt and mTOR, downstream targets of PI3K, in a dose-dependent manner.

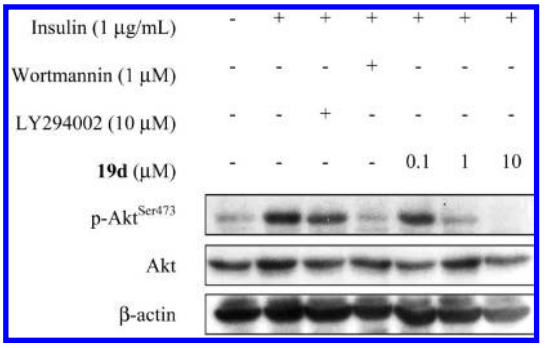

Figure 5. Inhibition of cellular PI3K pathway in Hep3B. Hep3B cells were treated with the indicated concentration of **19d** or 1 μM wortmannin or 10 μM LY294002A.

growth, cell viability was tested by 3-(4,5-dimethylthiazol-2-yl)-2,5-diphenyltetrazolium bromide (MTT) assay in T47D, SK-BR3, and MCF-7 human breast cancer cell cultures. Notably, compounds **19c**, **19d**, and **19o** showed potent antiproliferative effects at submicromolar concentration as shown in Table 4. The most potent compounds, **19f** and **19p** in enzyme assay were not very active in cell-based assay (IC_{50} >10 μM), which may be attributed to poor cellular permeability and water solubility. In this assay, natural product wortmannin inhibited cellular proliferation with an IC_{50} of 3.4 μM in T47D, showing approximately 5-fold less potency than **19c**.

3. MECHANISM STUDIES

The PI3K pathway plays a critical role in cell progression by promoting cell proliferation and inhibiting apoptosis. For selected inhibitors displaying potent enzymatic and cellular activity, the mechanism study of cancer cell death was assessed, followed in some cases by pharmacokinetic evaluation in vivo.

3.1. Cell-Signaling Effects. Activation of the PI3K pathway leads to phosphorylation of the Thr^{308} and Ser^{473} of Akt and subsequently to a number of downstream substrates such as IKK, GSK, and caspase-9. To ensure that the new series of compounds were inhibiting PI3K signaling in cells, **19d** was further profiled for its ability to suppress cellular biomarkers. After treatment with **19d** for 30 min, T47D cells were treated with 1 μg/mL insulin for 2 h to activate the PI3K pathway. Consistent with

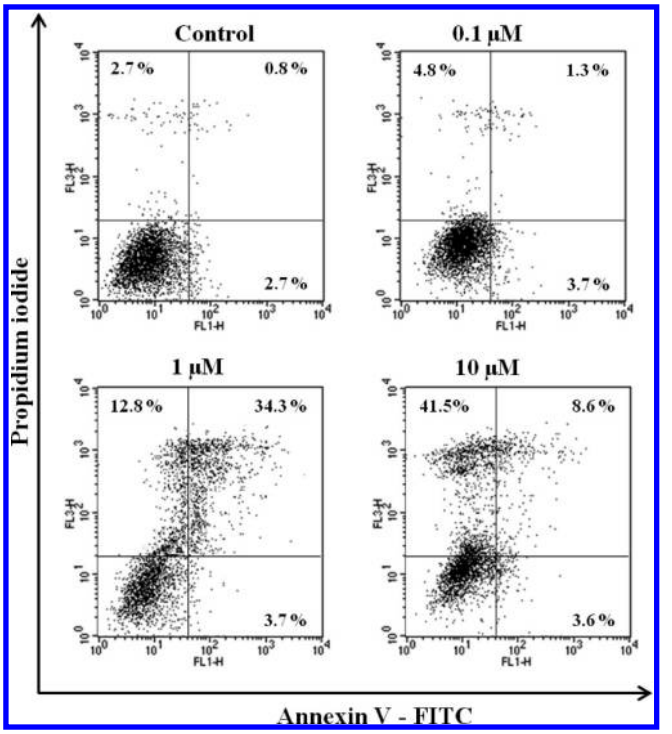

Figure 6. Compound **19d** promoted apoptosis of T47D breast cancer cells. T47D cells were treated with various concentrations of **19d** for 24 h, and apoptosis was determined by flow cytometric analysis using Annexin V-FITC and PI staining.

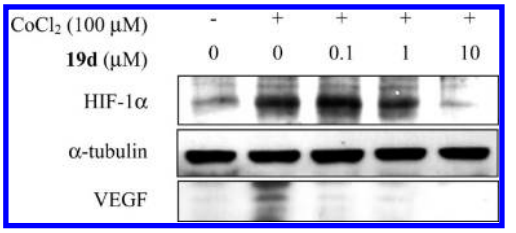

Figure 7. Effect of **19d** on the accumulation of HIF-1α. T47D cells were treated with various concentrations of **19d** for 30 min and 100 μM of $CoCl_2$ to hypoxic conditions for 6 h. Compound **19d** inhibited $CoCl_2$-induced HIF-1α and VEGF accumulation.

expectations for a potent PI3Kα inhibitor, **19d** strongly suppressed phosphorylation of Akt at the threonine 308 and serine 473 and its downstream m-TOR in a dose dependent manner (Figure 4). We also compared the suppression of PI3K signaling by **19d** with wortmannin and LY294002A as shown in Figure 5. Compound **19d** shows p-Akt reduction starting at 1 μM and is almost complete at 10 μM.

3.2. Apoptosis. Because compound **19d** successfully demonstrated the ability to inhibit p-Akt (at Ser^{473}) in T47D cancer cells, we further determined whether the inhibition of PI3Kα by **19d** induces apoptosis in cancer cells. The percentage of apoptotic cells was measured by the percentage of Annexin V-positive/PI-negative cells present after incubation with various concentrations of **19d** for 24 h. Exposure to 1 μM of **19d** resulted in 34.3% and 12.8% increases in apoptotic (Annexin V-positive/PI-Positive) and necrotic cells (Annexin V-negative/PI-positive), respectively. Exposure to 10 μM of **19d** resulted in a 41.5% increase in necrotic cells (Figure 6).

3.3. Effect on Angiogenesis. Angiogenesis is an essential process for tumor growth and metastasis, and activation of the PI3K pathway contributes to angiogenesis during tumor growth. Because HIF-1α is the major transcriptional modulator of angiogenic factors such as VEGF, we examined the effect of **19d** on the expression of hypoxia induced HIF-1α and VEGF to determine whether angiogenesis is suppressed by the inhibition of PI3Kα. After treatment with **19d** for 30 min, T47D cells were treated with the hypoxia mimicking agent $CoCl_2$ for 6 h. As shown in Figure 7, the HIF-1α expression under hypoxic condition was increased, whereas **19d** inhibited the hypoxia-induced HIF-1α expression in a dose-dependent manner. Also, we investigated the effects of **19d** on production of the hypoxia-induced VEGF. When cells were treated with **19d** under hypoxia conditions, the VEGF protein level was dramatically reduced as shown in Figure 7.

3.4. Cell Migration. The antiangiogenic activity of the imidazopyridine analogues was further evaluated using assays for a wound induced migration of human umbilical vein endothelial cells (HUVEC) and tubular formation. Because cell migration is the one of major processes underlying tube formation, we examined the effects of **19b** and **19d** on the migration of HUVECs. Cell migration was quantified by counting the number of HUVECs that migrated into the nonwounded region.[15] As shown in Figure 8, both **19b** and **19d** reduced the migration of HUVECs in a dose-dependent manner after 24 h. These results collectively suggest that these inhibitors suppress the HIF-1α accumulation and thus inhibit the migration of endothelial cells.[16]

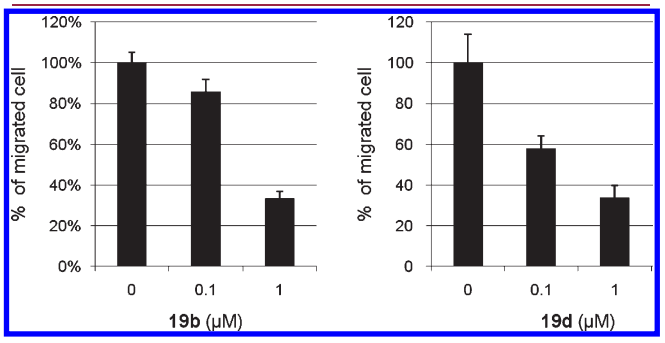

Figure 8. Inhibition of HUVEC migration by **19b** and **19d** in a wound-induced migration assay. Migration was quantified by counting the number of cells that moved beyond the reference line.

3.5. Tubular Network Formation. Next, the antiangiogenic effect on tube formation was analyzed by treating HUVEC with various concentrations of **19b** and **19d** (0.1, 1, and 10 μM).[17,18] While HUVECs were plated onto Matrigel where they aligned with one another and formed tubes resembling a capillary plexus, **19b** and **19d** produced significant inhibition of tubular network formation of the HUVECs on the Matrigel beds in a dose-dependent manner (Figure 9). The tubes were less extensive, thinner, and foreshortened when compared with the control.

4. Pharmacokinetic Data. Some of the leading compounds were subjected to pharmacokinetic studies in SD male rats. As shown in Table 5, pharmacokinetic parameters were determined after a single oral administration and intravenous injection. The selected compounds **19b** and **19d** demonstrated fair oral bioavailability (**19b**, 30.4%; **19d**, 24.2%) and desirable exposure

Table 5. Pharmacokinetic Profiles of Selected Compounds in SD Male Rats

parameters (iv)	19b	19d
$T_{1/2}$ (h)	2.4 ± 1.2	1.7 ± 0.4
AUC_{last} (μg.h/mL)	1.8 ± 0.9	16.9 ± 4.7
CL (L/kg/h)	3.58 ± 1.40	0.63 ± 0.19
Vss (L/kg)	12.23 ± 3.1	1.15 ± 0.1
F (%)	30.4	24.2

[a] The used vehicle was 40% PEG400 in saline and the pharmacokinetic parameters were determined after a single oral administration and intravenous injection (10 mg/kg) in SD male rats (n = 3).

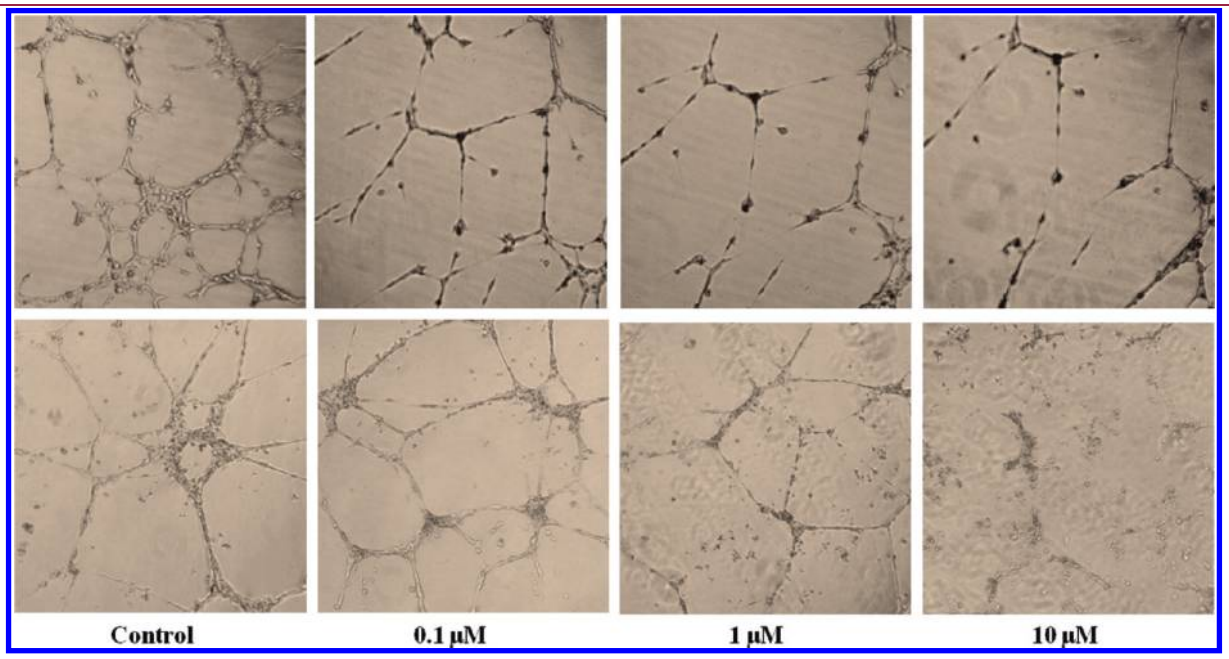

Figure 9. Effect of **19b** and **19d** on tubular network formation. Representative images depicting the formation of capillary-like tubular network formation of HUVEC by treatment with DMSO (control) and each inhibitor (up, **19b**; down **19d**).

levels (AUC) in the rats. Current efforts are focused on generating analogues with more suitable pharmacokinetic profiles.

5. CONCLUSION

We have designed and synthesized a new series of imidazo[1,2-*a*]pyridine derivatives as potent PI3Kα inhibitors utilizing the fragment-growing strategy. Through the exploration of the C3 and C6 position of imidazo[1,2-*a*]pyridines, we successfully developed the SAR profile around this series and found that some moieties (e.g., ester, nitrile, oxadiazole, tetrazole, and pyridine) at the C3 position profoundly influenced PI3Kα binding affinity, resulting in subnanomolar inhibitors with good antiproliferative cellular activity. Moreover, these inhibitors exhibited strong apototic and antiangiogenic effects by inhibiting VEGF expression. Further refinement of analogues and evaluation of in vivo antitumor efficacy is in progress.

6. EXPERIMENTAL SECTION

General Chemistry. Unless stated otherwise, reactions were performed in flame-dried glassware under a positive pressure of nitrogen using freshly distilled solvents. Analytical thin layer chromatography (TLC) was performed on precoated silica gel 60 F_{254} plates and visualization on TLC was achieved by UV light (254 and 354 nm). Flash column chromatography was undertaken on silica gel (400−630 mesh). ^{1}H NMR was recorded on 400 or 300 MHz, and chemical shifts were quoted in parts per million (ppm) referenced to the appropriate solvent peak or 0.0 ppm for tetramethylsilane. The following abbreviations were used to describe peak splitting patterns when appropriate: br = broad, s = singlet, d = doublet, t = triplet, q = quartet, m = multiplet, dd = doublet of doublet. Coupling constants, *J*, were reported in hertz unit (Hz). Chemical shifts were reported in ppm referenced to the center line of a triplet at 77.0 ppm of chloroform-*d*. Mass spectral data were obtained from the KAIST Basic Science Institute by using the EI method. If needed, products were purified via a Waters semipreparative HPLC equipped with an Agilent Prep-C18 reverse phase column (21.2 mm × 150 mm, 10 μm). The mobile phase was a mixture of MeOH (0.1% TFA) and H_2O (0.1% TFA). High performance liquid chromatography analyses for checking purity (>95% area) of synthesized compounds were performed on Waters HPLC equipped with a reverse phase column and by HRMS. All final compounds were found to have > 95% purity unless otherwise specified. Commercial grade reagents and solvents were used without further purification except as indicated below. Dichloromethane was distilled from calcium hydride. THF was distilled from sodium. Unless otherwise stated, all commercial reagents and solvents were used without additional purification.

Biological Assays and Methods. *PI3-Kinase.* The PI3K assay was performed using the Kinase-Glo Max luminescent kinase assay kit (Promega cat. no. V6073) which quantifies the amount of ADP produced by the PI3K reaction. In brief, an active PI3K (100 ng) was preincubated with compound for 5 min in kinase reaction buffer (25 mM MOPS [pH 7.0], 5 mM $MgCl_2$, and 1 mM EGTA) and 10 μg L-α-phosphatidylinositol (PI) (Sigma cat. no. P8443). Before addition of PI, it was sonicated with sonication buffer (25 mM MOPS [pH 7.0], 1 mM EGTA) in water for 20 min for allowing miscelle formation. Then reaction was started by the addition of 10 μM ATP and ran for 180 min. To terminate kinase reaction, same volume of Kinase-Glo Max buffer was added. After 10 min, the plates were then read on a GloMax plate reader for luminescence detection.

MTT assay. Cell viability was performed by a MTT assay. Briefly, T47D cells were plated at a density of 5×10^3 cells/well in 96-well plates for 24 h. Then, the medium was removed and cells were treated with either DMSO as a control or various concentrations of inhibitors. The final concentration of DMSO in the medium was ≤0.1% (v/v). After the cells were incubated for 482 h, 20 μL MTT solution (5 mg/mL) was added to each well for another 4 h at 37 °C. The formazan crystals that formed were dissolved in DMSO (100 μL/well) by constant shaking for 5 min. The plate was then read on a microplate reader at 540 nm. Three replicate wells were used for each analysis. The median inhibitory concentration (IC_{50}, defined as the drug concentration at which cell growth was inhibited by 50%) was assessed from the dose−response curves. To assess the effect of compounds on cell proliferation, T47D cells were cultured with compound (0.1−100 μM) for 48 h before MTT analysis.

N-(5-(3-Pyridyl)pyridin-3-yl)benzenesulfonamide (3a). To a solution of *N*-(5-bromopyridin-3-yl)benzenesulfonamide (110 mg, 0.31 mmol) in 1,4-dioxane/water (3/1) (5 mL) were added 3-pyridylboronic acid (38 mg, 0.31 mmol), K_2CO_3 (170 mg, 1.2 mmol), and $PdCl_2(PPh_3)_2$ (11 mg, 0.016 mmol). The resulting mixture was stirred at 100 °C for 3 h and then cooled to rt. After removal of the solvent, the residue was purified by flash column chromatography (MeOH:CH_2Cl_2, 1:20) to give **3a** as a white solid (32 mg, 33% yield). ^{1}H NMR ($CDCl_3$, 300 MHz) δ 7.39−7.58 (m, 4H), 7.76−7.85 (m, 4H), 8.25 (d, 1H, *J* = 2.5 Hz), 8.59 (d, 1H, *J* = 1.9 Hz), 8.67 (d, 1H, *J* = 4.8 Hz), 8.76 (d, 1H, *J* = 2.1 Hz). HPLC purity 99.1%.

N-(5-(4-Pyridyl)pyridin-3-yl)benzenesulfonamide (3b). Compound **3b** was prepared (41% yield) according to the procedure described for **3a**. ^{1}H NMR (MeOD-d_4, 300 MHz) δ 7.49−7.54 (m, 2H), 7.57−7.60 (m, 1H), 7.65 (m, 2H), 7.81 (m, 1H), 7.84 (m, 1H), 7.89 (m, 1H), 8.31 (m, 1H), 8.61 (m, 3H). HPLC purity 96.1%.

N-(5-(2-Aminopyrimidin-5-yl)pyridin-3-yl)benzenesulfonamide (3c). Compound **3c** was prepared from 5-bromopyrimidin-2-amine (30% yield) according to the procedure described for **9**. ^{1}H NMR (DMSO-d_6, 300 MHz) δ 6.93 (s, 2H), 7.54−7.63 (m, 4H), 7.80 (d, 2H, *J* = 6.8 Hz), 8.18 (s, 1H), 8.46 (d, 2H, *J* = 1.3 Hz), 8.50 (s, 1H), 10.63 (s, 1H). HPLC purity 96.9%.

N-(5-(1H-Pyrrolo[2,3-b]pyridin-5-yl)pyridin-3-yl)benzenesulfonamide (3d). Compound **3d** was prepared (56%), according to the procedure described for **3e**. ^{1}H NMR (DMSO- d_6, 300 MHz) δ 6.54 (d, 1H, *J* = 1.98 Hz), 7.58 (m, 4H), 7.73 (m, 1H), 7.82 (s, 1H), 7.84 (s, 1H), 8.15 (s, 1H), 8.25 (m, 1H), 8.38 (s, 1H), 8.60 (s, 1H), 10.60 (br, 1H), 11.80 (s, 1H).

N-(5-(Imidazo[1,2-a]pyridin-6-yl)pyridin-3-yl)benzenesulfonamide (3e). To a solution of 6-bromoimidazo[1,2-*a*]pyridine (160 mg, 0.83 mmol) in 1,4-dioxane/water (3:1) (5 mL) were added 5-(4,4,5,5-tetramethyl-1,3,2-dioxaborolan-2-yl)pyridin-3-amine (180 mg, 0.83 mmol), K_2CO_3 (460 mg, 3.3 mmol), and $PdCl_2(dppf)\cdot CH_2Cl_2$ (34 mg, 0.041 mmol). The resulting mixture was stirred at 100 °C for 12 h and then cooled to rt. After removal of the solvent, the residue was purified by flash column chromatography (MeOH:CH_2Cl_2, 1:20) to give the desired product (33 mg, 19% yield).

To a solution of above solid (20 mg, 0.10 mmol) and pyridine (12 μL, 0.14 mmol) in CH_2Cl_2 (5 mL) were added benzenesulfonyl chloride (15 μL, 0.16 mmol). The resulting reaction mixture was stirred at rt for 24 h and then concentrated in vacuo. The residue was purified by flash column chromatography (MeOH:CH_2Cl_2, 1:20) to give **3e** as a white solid (10 mg, 30% yield). ^{1}H NMR (DMSO-d_6, 300 MHz) δ 7.45 (d, 1H, *J* = 1.6 Hz), 7.57−7.64 (m, 5H), 7.66−7.83 (m, 3H), 8.00 (s, 1H), 8.25 (d, 1H, *J* = 2.2 Hz), 8.60 (d, 1H, *J* = 1.7 Hz), 8.92 (s, 1H), 10.75 (br, 1H). HRMS (EI+) *m*/*z* calcd for $C_{18}H_{14}N_4O_2S$ $[M + H]^+$, 351.0916; found, 351.0913. HPLC purity 96.6%.

N-(5-(3-Acetylimidazo[1,2-a]pyrimidin-6-yl)pyridin-3-yl)benzenesulfonamide (3f). Compound **3f** was prepared (71% yield) according to the procedure described for **3e** (steps 1−2). ^{1}H NMR (DMSO-d_6, 300 MHz) δ 2.61 (s, 3H), 7.60−7.65 (m, 3H), 7.82−7.87 (m, 3H), 8.36 (d, 1H, *J* = 2.4 Hz), 8.68 (d, 1H, *J* = 2.0 Hz), 8.83 (s, 1H), 9.10 (d, 1H, *J* = 2.6 Hz), 9.85 (d, 1H, *J* = 2.6 Hz), 10.84 (s, 1H). HRMS

(EI+) m/z calcd for $C_{19}H_{15}N_5O_3S$ $[M + H]^+$, 394.0975; found, 394.1016. HPLC purity 96.7%.

(E)-N′-(5-Bromopyridin-2-yl)-N,N-dimethylformimidamide (5). To a solution of **4** (1.7 g, 9.9 mmol) in MeOH (10 mL) was added 1,1-dimethoxy-*N*,*N*-dimethylmethaneamine (1.6 mL, 12 mmol). The resulting reaction mixture was refluxed at 70 °C for 6 h and then evaporated. The resulting mixture was subjected to recrystallization from hexane to give the desired product (2.2 g, 98% yield). ^{1}H NMR ($CDCl_3$, 300 MHz) δ 3.02 (s, 3H), 3.03 (s, 3H), 8.36 (s, 2H), 8.39 (s, 1H).

6-Bromoimidazo[1,2-a]pyridine-3-carbonitrile (6). To a solution of **5** (240 mg, 1.1 mmol) in *i*-PrOH (5 mL) were added $NaHCO_3$ (130 mg, 1.6 mmol) and bromoacetonitrile (92 μL, 1.3 mmol). The resulting reaction mixture was stirred at 100 °C for 12 h and then cooled to rt. After removal of the solvent, the residue was diluted with water and CH_2Cl_2. The organic layer was extracted with CH_2Cl_2, dried over $MgSO_4$, filtered, and then concentrated. The residue was recrystallized from ethanol to give **6** as a white solid (240 mg, 100% yield). ^{1}H NMR ($CDCl_3$, 300 MHz) δ 7.50 (d, 1H, J = 9.5 Hz), 7.65 (d, 1H, J = 9.5 Hz), 8.08 (s, 1H), 8.49 (s, 1H).

3-(6-Bromoimidazo[1,2-a]pyridin-3-yl)-5-methyl-1,2,4-oxadiazole (7). To a solution of **6** (1.1 g, 5.0 mmol) in EtOH (20 mL) were added triethylamine (1.4 mL, 10 mmol) and hydroxylamine hydrochloride (420 mg, 6.0 mmol). The resulting reaction mixture was stirred at rt for 15 h and then evaporated.

To a solution of resulting residue in 1,4-dioxane (20 mL) was added acetic anhydride (14 mL, 15 mmol). The reaction mixture was stirred at 120 °C for 21 h and then cooled to rt. After removal of the solvent, the residue was diluted with water and CH_2Cl_2 and neutralized to pH 8. The organic layer was extracted with CH_2Cl_2, dried over $MgSO_4$, filtered, and then concentrated. The residue was purified by flash column chromatography (MeOH:CH_2Cl_2, 1:40) to give **7** as a white solid (980 mg, 70% yield). ^{1}H NMR ($CDCl_3$, 300 MHz) δ 2.67 (s, 3H), 7.42 (d, 1H, J = 9.5 Hz), 7.62 (d, 1H, J = 9.4 Hz), 8.30 (s, 1H), 9.29 (s, 1H).

6-Bromo-3-iodoimidazo[1,2-a]pyridine (12). Compound **4** (2.8 g, 16 mmol), chloroacetaldehyde (1.5 mL, 19 mmol), $NaHCO_3$ (2.7 g, 32 mmol), and *i*-PrOH (10 mL) were combined in a sealed tube and heated to 100 °C. After 24 h, the mixture was cooled to rt and concentrated under reduced pressure. The residue was diluted with CH_2Cl_2, washed with water and brine, and the combined aqueous layers were back-extracted with CH_2Cl_2. The combined extracts were dried over $MgSO_4$ and concentrated. The residue was subjected to recrystallization from hexane to give the desired product (2.5 g, 80% yield). ^{1}H NMR ($CDCl_3$, 300 MHz) δ 6.98 (d, 1H, J = 9.5 Hz), 7.29 (d, 1H, J = 9.4 Hz), 7.31 (s, 1H), 7.44 (s, 1H), 8.07 (s, 1H).

To the above resulting solid (1.1 g, 5.4 mmol) in anhydrous acetonitrile (15 mL) was added *N*-iodosuccinimide (1.2 g, 5.4 mmol). The resulting mixture was stirred at rt for 12 h. The crude product was collected by filtration and treated with acetonitrile to provide **12** as a white solid (1.5 g, 85% yield). ^{1}H NMR ($CDCl_3$, 300 MHz) δ 7.28 (d, 1H, J = 9.4 Hz), 7.49 (d, 1H, J = 9.5 Hz), 7.68 (s, 1H), 8.26 (s, 1H).

6-Bromo-3-(pyridin-3-yl)imidazo[1,2-a]pyridine (13). To a solution of **12** (270 mg, 0.82 mmol) were added 3-pyridylboronic acid (190 mg, 0.91 mmol), K_2CO_3 (450 mg, 3.3 mmol), and $PdCl_2(dppf)\cdot CH_2Cl_2$ (67 mg, 0.082 mmol). The resulting mixture was stirred at 80 °C for 4 h and then cooled to rt. After removal of the solvent, the residue was purified by flash column chromatography (MeOH:CH_2Cl_2, 1:20) to give **13** as a white solid (160 mg, 73% yield). ^{1}H NMR ($CDCl_3$, 300 MHz) δ 7.27−7.31 (m, 1H), 7.48−7.50 (m, 1H), 7.59 (d, 1H, J = 9.6 Hz), 7.74 (s, 1H), 7.87 (d, 1H, J = 6.1 Hz), 8.38 (s, 1H), 8.68−8.70 (m, 1H), 8.83 (d, 1H, J = 2.0 Hz).

Ethyl 6-Bromoimidazo[1,2-a]pyridine-3-carboxylate (15). A mixture of ethyl formate (3.2 mL, 39 mmol) and ethyl chloroacetate (4.2 mL, 39 mmol) was added to a suspension of potassium *t*-butoxide (4.8 g, 39 mmol) and DIPE (20 mL) at 0 °C, and the whole was stirred for 24 h at rt. The resulting precipitate was collected by filtration to give ethyl 2-chloro-3-oxopropanoate potassium salt as an orange solid (4.9 g, 65% yield).

To a solution of conc H_2SO_4 (5 drops) in EtOH (5 mL) were added **4** (1.4 g, 8.3 mmol) and ethyl 2-chloro-3-oxopropanoate potassium salt (4.9 g, 26 mmol) in a sealed tube. The reaction vessel was purged with nitrogen gas, sealed, and heated to 90 °C. After 21 h, the resultant slurry was cooled to rt, filtered, and concentrated under reduced pressure. The residue was diluted with EtOAc, washed with 1N NaOH followed by brine, and the combined aqueous layers were back-extracted with EtOAc. The combined extracts were dried over $MgSO_4$ and concentrated under reduced pressure. The residue was purified by flash column chromatography on silica gel using CH_2Cl_2 to give **15** as a yellow solid (1.7 g, 76% yield). ^{1}H NMR ($CDCl_3$, 300 MHz) δ 1.39 (t, 3H, J = 7.1 Hz), 4.39 (dd, 2H, J = 7.1, 10.7 Hz), 7.44 (d, 1H, J = 9.5 Hz), 7.59 (d, 1H, J = 9.6 Hz), 8.22 (s, 1H), 9.45 (s, 1H).

4-(6-Bromoimidazo[1,2-a]pyridin-3-yl)morpholine (17). Benzotriazole (1.3 g, 11 mmol) and morpholine (0.93 mL, 11 mmol) were stirred in ethanol (15 mL) at RT for 5 min. Glyoxal (0.61 mL, 5.3 mmol) was added to the reaction mixture, and the stirring was continued overnight at rt. The resulting solid was collected by filtration, washed with ethanol, and dried in vacuo to give an off-white solid (1.8 g, 77% yield).

To a solution of resulting residue (8.0 g, 19 mmol) in 1,2-dichloroethane (30 mL) was added **4** (3.2 g, 19 mmol). The resulting mixture was stirred at 100 °C for 2 h and then cooled to rt. Powdered KOH (3.4 g, 61 mmol) was added to the solution and the reaction mixture was stirred at rt for 0.5 h. Then the solid was filtered out and washed with chloroform. After removal of the solvent, the residue was separated by flash column chromatography (EtOAc:hexane, 1:3) to give **17** as a white solid (2.3 g, 44% yield). ^{1}H NMR ($CDCl_3$, 300 MHz) δ 2.97−3.00 (m, 4H), 3.83−3.86 (m, 4H), 7.12 (d, 1H, J = 8.5 Hz), 7.26 (s, 1H), 7.39 (d, 1H, J = 7.0 Hz), 8.06 (s, 1H).

N-(5-(3-Acetylimidazo[1,2-a]pyridin-6-yl)pyridin-3-yl)benzenesulfonamide (19a). Compound **19a** was prepared (71% yield), according to the procedure described for **3e** (steps 1−2). ^{1}H NMR (DMSO-d_6, 300 MHz) δ 2.60 (s, 3H), 7.60−7.65 (m, 3H), 7.78 (m, 1H), 7.84−7.97 (m, 4H), 8.34 (d, 1H, J = 2.3 Hz), 8.62 (d, 1H, J = 2.0 Hz), 8.68 (s, 1H), 9.71 (s, 1H), 10.82 (s, 1H). HRMS (EI+) m/z calcd for $C_{20}H_{16}N_4O_3S$ $[M + Na]^+$, 415.0841; found, 415.0842. HPLC purity 100%.

N-(5-(3-Cyanoimidazo[1,2-a]pyridin-6-yl)pyridin-3-yl)benzenesulfonamide (19b). Compound **19b** was prepared from **6** to give an off-white solid (32% yield) according to the procedure described for **3e**, using *N*-(5-(4,4,5,5-tetramethyl-1,3,2-dioxaborolan-2-yl)pyridin-3-yl)-benzenesulfonamide. ^{1}H NMR (DMSO-d_6, 300 MHz) δ 7.56−7.65 (m, 3H), 7.79−7.85 (m, 4H), 7.95 (d, 1H, J = 9.4 Hz), 8.31 (s, 1H), 8.49 (s, 1H), 8.70 (s, 1H), 8.79 (s, 1H), 10.74 (s, 1H). HRMS (EI+) m/z calcd for $C_{19}H_{13}N_5O_2S$ $[M + H]^+$, 376.0869; found, 376.0862. HPLC purity 97.2%.

Ethyl 6-(5-(Phenylsulfonamido)pyridin-3-yl)imidazo[1,2-a]-pyridine-3-carboxylate (19c). Compound **19c** was prepared from **15** (26% yield), according to the procedure described for **3e** (step 1). ^{1}H NMR (DMSO-d_6, 300 MHz) δ 1.36 (t, 3H, J = 7.1 Hz), 4.40 (q, 2H, J = 7.1 Hz), 7.76−7.63 (m, 3H), 7.79−7.86 (m, 4H), 7.92 (d, 1H, J = 9.4 Hz), 8.33 (s, 1H), 8.34 (s, 1H), 8.62 (d, 1H, J = 1.9 Hz), 9.38 (s, 1H), 10.81 (br, 1H). HRMS (EI+) m/z calcd for $C_{21}H_{18}N_4O_4S$ $[M + H]^+$, 423.1128; found, 423.1123. HPLC purity 99.2%.

N-(5-(3-(5-Methyl-1,2,4-oxadiazol-3-yl)imidazo[1,2-a]pyridin-6-yl)pyridin-3-yl)benzenesulfonamide (19d). Compound **19d** was prepared from **7** (64% yield) according to the procedure described for **3e** (steps 1−2). ^{1}H NMR (DMSO-d_6, 300 MHz) δ 2.73 (s, 3H),

7.59−7.61 (m, 3H), 7.81 (m, 2H), 7.87 (d, 2H, J = 6.5 Hz), 7.95 (d, 1H, J = 9.4 Hz), 8.33 (d, 1H, J = 2.4 Hz), 8.37 (s, 1H), 8.61 (s, 1H), 9.21 (s, 1H). HRMS (EI+) m/z calcd for $C_{21}H_{16}N_6O_3S$ $[M + H]^+$, 433.1084; found, 433.1078. HPLC purity 98.6%.

N-(5-(3-(1H-Pyrazol-3-yl)imidazo[1,2-a]pyridin-6-yl)pyridin-3-yl)-benzenesulfonamide (19e). Compound **19a** (59 mg, 0.15 mmol) in 1,1-dimethoxy-*N*,*N*-dimethylmethaneamine (3 mL, 23 mmol) was refluxed at 100 °C for 16 h, and then the solvent was evaporated. To a resultant residue in EtOH (10 mL) was added hydrazine hydrate (17 μL, 0.33 mmol). The resulting reaction mixture was stirred at 80 °C for 7 h. After removal of the solvent, the residue was purified by flash column chromatography (MeOH:CH_2Cl_2, 1:20) to give **19e** as a white solid (12 mg, 19% yield). ^{1}H NMR (DMSO-d_6, 300 MHz) δ 6.85 (d, 1H, J = 2.3 Hz), 7.45−7.60 (m, 6H), 7.82 (s, 1H), 7.98−8.00 (m, 2H), 8.03 (s, 1H), 8.16 (d, 1H, J = 8.2 Hz), 8.36 (s, 1H), 8.41 (d, 1H, J = 2.4 Hz), 8.78(s, 1H), 10.1 (s, 1H). HRMS (EI+) m/z calcd for $C_{21}H_{16}N_6O_2S$ $[M + H]^+$, 417.1134; found, 417.1122. HPLC purity 97.5%.

N-(5-(3-(2H-Tetrazol-5-yl)imidazo[1,2-a]pyridin-6-yl)pyridin-3-yl)-benzenesulfonamide (19f). To a solution of **19b** (47 mg, 0.11 mmol) and sodium azide (15 mg, 0.22 mmol) in DMF (5 mL) was added $CdCl_2$ (4.0 mg, 0.023 mmol). The resulting reaction mixture was stirred at 80 °C for 12 h. After removal of solvent, the residue was purified by flash column chromatography (MeOH:CH_2Cl_2, 1:3) to give **19f** as a white solid (19 mg, 40% yield). ^{1}H NMR (DMSO-d_6, 300 MHz) δ 7.52−7.66 (m, 5H), 7.73 (s, 1H), 7.76−7.78 (m, 1H), 7.91 (dd, 2H, J = 1.7, 7.1 Hz), 8.01 (s, 1H), 8.31 (d, 1H, J = 2.2 Hz), 8.55 (s, 1H), 9.91 (s, 1H), 10.80 (br, 1H). HRMS (EI+) m/z calcd for $C_{19}H_{14}N_8O_2S$ $[M + Na]^+$, 441.0858; found, 441.0834. HPLC purity 98.6%.

N-(5-(3-Morpholinoimidazo[1,2-a]pyridin-6-yl)pyridin-3-yl)-benzenesulfonamide (19g). Compound **19g** was prepared from **17** (46% yield) according to the procedure described for **3e** (steps 1−2). ^{1}H NMR (DMSO-d_6, 300 MHz) δ 3.01 (t, 4H, J = 4.5 Hz), 3.80 (t, 4H, J = 4.4 Hz), 7.36 (m, 2H), 7.57−7.72 (m, 4H), 7.80 (t, 1H), 7.83 (d, 2H, J = 6.8 Hz), 8.29 (d, 2H, J = 2.4 Hz), 8.64 (d, 1H, J = 1.9 Hz), 11.75 (br, 1H). HRMS (EI+) m/z calcd for $C_{22}H_{21}N_5O_3S$ $[M + H]^+$, 436.1444; found, 436.1450. HPLC purity 98.60%.

N-(5-(3-Phenylimidazo[1,2-a]pyridin-6-yl)pyridin-3-yl)benzenesulfonamide (19h). Compound **19h** was prepared (27%), according to the procedure described for **19b**. ^{1}H NMR (DMSO-d_6, 300 MHz) δ 7.47−7.61 (m, 7H), 7.69 (t, 1H, J = 2.2 Hz), 7.73 (s, 1H), 7.76−7.82 (m, 5H), 8.28 (d, 1H, J = 2.39 Hz), 8.58 (s, 1H), 8.61 (d, 1H, J = 1.93 Hz), 10.70 (s, 1H). HPLC purity 99.1%.

N-(5-(3-(3-Cyanophenyl)imidazo[1,2-a]pyridin-6-yl)pyridin-3-yl)-benzenesulfonamide (19i). Compound **19i** was prepared (23% yield), according to the procedure described for **3e** (steps 1−2). ^{1}H NMR (DMSO-d_6, 300 MHz) δ 7.44−7.53 (m, 5H), 7.70−7.78 (m, 7H), 7.95 (m, 1H), 8.06 (s, 1H), 8.22 (d, 1H, J = 2.4 Hz), 8.48 (d, 1H, J = 2.0 Hz), 8.55 (s, 1H). HRMS (EI+) m/z calcd for $C_{25}H_{17}N_5O_2S$ $[M + H]^+$, 452.1182; found, 452.1203. HPLC purity 98.7%.

N-(5-(3-(Pyridin-3-yl)imidazo[1,2-a]pyridin-6-yl)pyridin-3-yl)-benzenesulfonamide (19j). Compound **19j** was prepared (36% yield) according to the procedure described for **3e** (steps 1−2). ^{1}H NMR (DMSO-d_6, 300 MHz) δ 6.86−6.91 (m, 5H), 7.18−7.25 (m, 5H), 7.45 (m, 1H), 7.68 (d, 1H, J = 2.4 Hz), 7.83−7.84 (m, 1H), 7.87 (d, 1H, J = 2.0 Hz), 8.10 (m, 1H), 8.25 (s, 1H). HRMS (EI+) m/z calcd for $C_{23}H_{17}N_5O_2S$ $[M + Na]^+$, 450.1001; found, 450.1011. HPLC purity 96.0%.

N-(5-(3-(Pyridin-4-yl)imidazo[1,2-a]pyridin-6-yl)pyridin-3-yl)-benzenesulfonamide (19k). Compound **19k** was prepared (31% yield) according to the procedure described for **3e** (steps 1−2). ^{1}H NMR (DMSO-d_6, 300 MHz) δ 7.54−7.61 (m, 4H), 7.74 (s, 1H), 7.81 (d, 4H, J = 6.0 Hz), 7.85 (s, 1H), 8.07 (s, 1H), 8.28 (d, 1H, J = 2.3 Hz), 8.65 (s, 1H), 8.69 (d, 2H, J = 6.1 Hz), 8.80 (s, 1H). HPLC purity 95.4%.

6-(6-Amino-5-(morpholinosulfonyl)pyridin-3-yl)imidazo[1,2-a]-pyridine-3-carbonitrile (19l). Compound **19l** was prepared from **7** (4% yield) according to the procedure described for **3e**, using 3-(morpholinosulfonyl)-5-(4,4,5,5-tetramethyl-1,3,2-dioxaborolan-2-yl)-pyridin-2-amine. ^{1}H NMR (DMSO-d_6, 300 MHz) δ 3.07 (m, 4H), 3.60 (m, 4H), 6.90 (br, 2H), 7.77 (s, 2H), 7.98 (d, 1H, J = 2.2 Hz), 8.35 (s, 1H), 8.60 (d, 1H, J = 2.4 Hz), 9.66 (s, 1H). HPLC purity 96.4%.

6-(6-Amino-5-(morpholinosulfonyl)pyridin-3-yl)imidazo[1,2-a]-pyridine-3-carbonitrile (19m). Compound **19m** was prepared from **17** (14% yield), according to the procedure described for **3e** (step 1), using 3-(morpholinosulfonyl)-5-(4,4,5,5-tetramethyl-1,3,2-dioxaborolan-2-yl)-pyridin-2-amine. ^{1}H NMR (DMSO-d_6, 300 MHz) δ 3.07 (m, 4H), 3.60 (m, 4H), 6.90 (br, 2H), 7.77 (s, 2H), 7.98 (d, 1H, J = 2.2 Hz), 8.35 (s, 1H), 8.60 (d, 1H, J = 2.4 Hz), 9.66 (s, 1H). HPLC purity 96.4%.

N-(5-(3-Cyanoimidazo[1,2-a]pyridin-6-yl)pyridin-3-yl)-2,4-difluoro-benzenesulfonamide (19n). Compound **19n** was prepared from **6** (16% yield), according to the procedure described for **3e** (step 1), using 2,4-difluoro-*N*-(5-(4,4,5,5-tetramethyl-1,3,2-dioxaborolan-2-yl)pyridin-3-yl)benzenesulfonamide. ^{1}H NMR (DMSO-d_6, 300 MHz) δ 7.24−7.29 (m, 1H), 7.50−7.56 (m, 1H), 7.80−7.83 (m, 2H), 7.94−8.05 (m, 2H), 8.33 (s, 1H), 8.50 (s, 1H), 8.67 (s, 1H), 8.78 (s, 1H), 11.15 (br, 1H). HRMS (EI+) m/z calcd for $C_{19}H_{11}F_2N_5O_2S$ $[M + H]^+$, 412.0681; found, 412.0679. HPLC purity 97.8%.

2,4-Difluoro-N-(5-(3-(5-methyl-1,2,4-oxadiazol-3-yl)imidazo[1,2-a]pyridin-6-yl)pyridin-3-yl)benzenesulfonamide (19o). Compound **19o** was prepared from **7** (60% yield), according to the procedure described for **3e** (steps 1−2), using 2,4-difluorobenzenesulfonyl chloride. ^{1}H NMR(DMSO-d_6, 300 MHz) δ 2.73 (s, 3H), 7.29(t, 1H, J = 3.3 Hz), 7.55 (t, 1H, J = 2.9 Hz), 7.82 (m, 2H), 7.96 (d, 1H, J = 3.1 Hz), 8.05 (dd, 1H, J = 2.9, 4.9 Hz), 8.38 (d, 2H, J = 1.2 Hz), 8.65 (s, 1H), 9.21 (s, 1H), 11.25 (s, 1H). HRMS (EI+) m/z calcd for $C_{21}H_{14}F_2N_6O_3S$ $[M + H]^+$, 469.0895; found, 469.0907. HPLC purity 100%.

N-(5-(3-(2H-Tetrazol-5-yl)imidazo[1,2-a]pyridin-6-yl)pyridin-3-yl)-2,4-difluorobenzenesulfonamide (19p). Compound **19p** was prepared from **19n** (26% yield) according to the procedure described for **19f**. ^{1}H NMR (DMSO-d_6, 300 MHz) δ 7.13 (d, 1H, J = 8.4 Hz), 7.25 (d, 1H, J = 9.3 Hz), 7.80−7.83 (m, 2H), 7.90−7.97 (m, 2H), 8.34 (s, 1H), 8.49 (s, 1H), 8.69 (s, 1H), 8.77 (s, 1H), 11.07 (br, 1H). HPLC purity 95.5%.

3,5-Difluoro-N-(5-(3-(5-methyl-1,2,4-oxadiazol-3-yl)imidazo[1,2-a]-pyridin-6-yl)pyridin-3-yl)benzenesulfonamide (19q). Compound **19q** was prepared from **7** (50% yield), according to the procedure described for **3e**, using 3,5-difluorobenzenesulfonyl chloride. ^{1}H NMR (DMSO-d_6, 300 MHz) δ 2.71 (s, 3H), 7.53(m, 2H), 7.62 (m, 1H), 7.82 (m, 2H), 7.95 (d, 1H, J = 3.1 Hz), 8.36 (s, 1H), 8.38 (d, 1H, J = 7.8 Hz), 8.70 (d, 1H, J = 6.5 Hz), 9.22 (s, 1H).

AUTHOR INFORMATION

Corresponding Author

*For S.H.: phone, (+82) 42-350-2811; fax, (+82) 42-350-2810; E-mail, hongorg@kaist.ac.kr. For S.-S.H.: phone, (+82) 32-890-3683; fax, (+82) 32-890-2462; E-mail, hongs@inha.ac.kr.

Author Contributions

§These authors contributed equally to this work

ACKNOWLEDGMENT

This research was supported by National Research Foundation of Korea (NRF) through general research grants (NRF-2010-0015340 and 2010-0022179).

ABBREVIATIONS USED

HIF-1, hypoxia-inducible factor; VEGF, vascular endothelial growth factor; PI3K, phosphoinositide 3-kinase; PIP2, phosphatidylinositol

4,5-bisphosphate; PIP3, phosphatidylinositol 3,4,5-trisphosphate; RTK, receptor protein tyrosine kinase; PTEN, phosphatase and tensin homologue; SAR, structure−activity relationships; ATP, adenosine-5′-triphosphate; MTT, 3-(4,5-dimethylthiazol-2-yl)-2,5-diphenyltetrazolium bromide; GSK3, glycogen synthase kinase 3; HUVEC, human umbilical vein endothelial cells; DMF, *N*,*N*-dimethylformamide; DIPE, diisopropyl ether

■ REFERENCES

(1) Kim, K. J.; Li, B.; Winer, J.; Armanini, M.; Gillett, N.; Phillips, H. S.; Ferrara, N. Inhibition of vascular endothelial growth factor-induced angiogenesis suppresses tumour growth in vivo. *Nature* **1993**, *362*, 841–844.

(2) Graupera, M.; Guillermet-Guibert., J.; Foukas, L. C.; Phng, L. K.; Cain, R. J.; Salpekar, A.; Pearce, W.; Meek, S.; Millan, J.; Cutillas, P. R.; Smith, A. J. H.; Ridley, A. J.; Ruhrberg, C.; Gerhardt, H.; Vanhaesebroeck, B. The catalytic subunits of class IA phosphoinositide 3-kinases (PI3K) are activated by distinct signals and have discrete roles in angiogenesis and vascular remodeling. *Nature* **2008**, *453*, 662–666.

(3) Liang, S.; Yang, N.; Pan, Y.; Deng, S.; Lin, X.; Yang, X.; Katsaros, D.; Roby, K. F.; Hamilton, T. C.; Connolly, D. C.; Coukos, G.; Zhang, L. The Oncogene Phosphatidylinositol 3′-Kinase Catalytic Subunit α Promotes Angiogenesis via Vascular Endothelial Growth Factor in Ovarian Carcinoma. *Cancer Res.* **2003**, *63*, 4225–4231.

(4) Vanhaesebroeck, B.; Leevers, S. J.; Khatereh, A.; Timms, J.; Katso, R.; Driscoll, P. C.; Woscholski, R.; Parker, P. J.; Waterfield, M. D. Synthesis and function of 3-phosphorylated inositol lipids. *Annu. Rev. Biochem.* **2001**, *70*, 535–602.

(5) (a) Parsons, D. W.; Wang, T.-L.; Samuels, Y.; Bardelli, A.; Cummins, J. M.; DeLong, L.; Silliman, N.; Ptak, J.; Szabo, S.; Willson, J. K.; Markowitz, S.; Kinzler, K. W.; Vogelstein, B.; Lengauer, C.; Velculescu, V. E. Colorectal cancer: mutations in a signalling pathway. *Nature* **2005**, *436*, 792. (b) Kang, S.; Bader, A. G.; Vogt, P. K. Phosphatidylinositol 3-kinase mutations identified in human cancer are oncogenic. *Proc. Natl. Acad. Sci. U.S.A.* **2005**, *102*, 802–807. (c) Fan, Q.-W.; Knight, A. A.; Goldenberg, D. D.; Yu, W.; Mostov, K. E.; Stokoe, D.; Shokat, K. M.; Weiss, W. A. A dual PI3 kinase/mTOR inhibitor reveals emergent efficacy in glioma. *Cancer Cell* **2006**, *9*, 341–349. (d) Ward, S.; Sotsios, Y.; Dowden, J.; Bruce, I.; Finan, P. Targeting the gatekeeper residue in phosphoinositide 3-kinases. *Chem. Biol.* **2003**, *10*, 207. (e) Ward, S. G.; Finan, P. Isoform-specific phosphoinositide 3-kinase inhibitors as therapeutic agents. *Curr. Opin. Pharmacol.* **2003**, *3*, 426–436.

(6) Skinner, H. D.; Zheng, J. Z.; Fang, J.; Agani, F.; Jiang, B. H. Vascular endothelial growth factor transcriptional activation is mediated by hypoxia inducible factor 1alpha, HDM2, and p70S6K1 in response to phosphatidylinositol 3-kinase/AKT signalling. *J. Biol. Chem.* **2004**, *279*, 45643–45651.

(7) Jiang, B. H.; Zheng, J. Z.; Aoki, M.; Vogt, P. K. Phosphatidylinositol 3-kinase signaling mediates angiogenesis and expression of vascular endothelial growth factor in endothelial cells. *Proc. Natl. Acad. Sci. U.S.A.* **2000**, *97*, 1749–1753.

(8) Hung, A. W.; Silvestre, H. L.; Wen, S.; Ciulli, A.; Blundell, T. L.; Abell, C. Application of fragment growing and fragment linking to the discovery of inhibitors of *Mycobacterium tuberculosis* pantothenate synthetase. *Angew. Chem., Int. Ed. Engl.* **2009**, *48*, 8452–8456.

(9) (a) Li, Q.; Woods, K. W.; Zhu, G.-D.; Fischer, J. P.; Gong, J.; Li, T.; Gandhi, V.; Thomas, S. A.; Packard, G.; Song, X.; Abrams, J. N.; Diebold, R.; Dinges, J.; Hutchins, C.; Stoll, V. S.; Rosenberg, S. H.; Giranda, V. L. Preparation of pyridine derivatives as protein kinase inhibitors. 3-(phenyl-alkoxy)-5-(phenyl)-pyridine derivatives and related compounds as kinase inhibitors for the treatment of cancer PCT Int. Appl. WO 2003051366, 2003. (b) Booker, S.; D'Angelo, N.; D'Amico, D. C.; Kim, T.-S.; Liu, L.; Meagher, K.; Norman, M. H.; Panter, K.; Schenkel, L. B.; Smith, A. L.; Tamayo, N. A.; Whittington, D. A.; Xi, N.; Yang, K. Preparation of 2-aminobenzothiazole derivatives as phosphoinositide 3-kinase (PI3 kinase) modulators. PCT Int. Appl. WO 2009017822, 2009. (c) Bo, Y. Y.; Booker, S.; Bryan, M.; Deak, H. L.; Liu, L.; Andrews, K.; Nishimura, N.; Norman, M. H.; Panter, K.; Schenkel, L.; Siegmund, A. C.; Tamayo, N. A.; Yang, K. Heteroarylpyridine derivatives as inhibitors of PI3 kinase and their preparation and use in the treatment of cancer. PCT Int. Appl. WO 2009155121, 2009. (d) Hamblin, J. N.; Jones, P. S.; Keeling, S. E.; Le, J.; Mitchell, C. J.; Parr, N. J. Preparation of oxazole-substituted indazole derivatives for use as PI3-kinase inhibitors. PCT Int. Appl. WO 2010125082. 2010. (e) Knight, S. D.; Adams, N. D.; Burgess, J. L.; Chaudhari, A. M.; Darcy, M. G.; Donatelli, C. A.; Luengo, J. I.; Newlander, K. A.; Parrish, C. A.; Ridgers, L. H.; Sarpong, M. A.; Schmidt, S. J.; Van Aller, G. S.; Carson, J. D.; Diamond, M. A.; Elkins, P. A.; Gardiner, C. M.; Garver, E.; Gilbert, S. A.; Gontarek, R. R.; Jackson, J. R.; Kershner, K. L.; Luo, L.; Raha, K.; Sherk, C. S.; Sung, C. M.; Sutton, D.; Tummino, P. J.; Wegrzyn, R. J.; Auger, K. R.; Dhanak, D. Discovery of GSK2126458, a Highly Potent Inhibitor of PI3K and the Mammalian Target of Rapamycin. *ACS Med. Chem. Lett.* **2010**, *1*, 39–43. (f) Hong, S.; Lee, S.; Kim, B.; Lee, H.; Hong, S.-S.; Hong, S. Discovery of new azaindole-based PI3Kα inhibitors: apoptotic and antiangiogenic effect on cancer cells. *Bioorg. Med. Chem. Lett.* **2010**, *20*, 7212–7215.(g) Adams, N. D.; Darcy, M. G.; Johnson, N. W.; Kasparec, J.; Knight, S. D.; Newlander, K. A.; Peng, X.; Ridgers, L. H. Pyridosulfonamide derivatives as PI3 kinase inhibitors. PCT Int. Appl. WO2009055418A1 2009.

(10) (a) Barile, E; De, S. K.; Carlson, C. B.; Chen, V.; Knutzen, C.; Riel-Mehan, M.; Yang, L.; Dahl, R.; Chiang, G.; Pellecchia, M. Design, Synthesis, and Structure−Activity Relationships of 3-Ethynyl-1*H*-indazoles as Inhibitors of the Phosphatidylinositol 3-Kinase Signaling Pathway. *J. Med. Chem.* **2010**, *53*, 8368–8375. (b) Kim, D.; Jun, H.; Lee, H.; Hong, S.-S.; Hong, S. Development of New Fluorescent Xanthines as Kinase Inhibitors. *Org. Lett.* **2010**, *12*, 1212–1215.

(11) Hayakawa, M.; Kawaguchi, K.; Kaizawa, H.; Koizumi, T.; Ohi-shi, T.; Yamano, M.; Okada, M.; Ohta, M.; Tsukamoto, S.; Raynaud, F. I.; Parker, P.; Workmanb, P.; Waterfield, M. D. Synthesis and biological evaluation of sulfonylhydrazone-substituted imidazo[1,2-*a*]pyridines as novel PI3 kinase p110α inhibitors. *Bioorg. Med. Chem.* **2007**, *15*, 5837–5844.

(12) (a) A homology model of p110α was generated based on the coordinates of a p110γ crystal structure in complex with staurosporine (PDB code: 1E8Z) as the template using the program MODELER. Subsequent docking studies were performed using AutoDock 4.0. Docking studies were either performed without constraints or with a hydrogen bonding constraint to the backbone-NH of Val851. (b) Cherian, P. T.; Koikov, L. N.; Wortman, M. D.; Knittel, J. J. Exploring the PI3K alpha and gamma binding sites with 2,6-disubstituted isonicotinic derivatives. *Bioorg. Med. Chem. Lett.* **2009**, *19*, 2215–2219.

(13) Maira, S.-M.; Stauffer, F.; Brueggen, J.; Furet, P.; Schnell, C.; Fritsch, C.; Brachmann, S.; Chene, P.; Pover, A. D.; Schoemaker, K.; Fabbro, D.; Gabriel, D.; Simonen, M.; Murphy, L.; Finan, P.; Sellers, W.; Garcıa-Echeverrıa, C. Identification and characterization of NVP-BEZ235, a new orally available dual phosphatidylinositol 3-kinase/mammalian target of rapamycin inhibitor with potent in vivo antitumor activity. *Mol. Cancer Ther.* **2008**, *7*, 1851–1863.

(14) Folkes, A. J.; Ahmadi, K; Alderton, W. K.; Alix, S; Baker, S. J.; Box, G.; Chuckowree, I. S.; Clarke, P. A.; Depledge, P.; Eccles, S. A.; Friedman, L. S.; Hayes, A.; Hancox, T. C.; Kugendradas, A.; Lensun., L.; Moore, P.; Olivero, A. G.; Pang, J.; Patel, S.; Pergl-Wilson, G. H.; Raynaud, F. I.; Robson, A.; Saghir, N.; Salphati, L.; Sohal, S.; Ultsch, M. H.; Valenti, M.; Wallweber, H. J. A.; Wan, N. C.; Wiesmann, C.; Workman, P.; Zhyvoloup, A.; Zvelebil, M. J.; Shuttleworth, S. J. The identification of 2-(1*H*-indazol-4-yl)-6-(4-methanesulfonyl-piperazin-1-ylmethyl)-4-morpholin-4-yl-thieno[3,2-*d*]pyrimidine (GDC-0941) as a potent, selective, orally bioavailable inhibitor of class I PI3 kinase for the treatment of cancer. *J. Med. Chem.* **2008**, *51*, 5522–5532.

(15) Sato, Y.; Rifkin, D. B. Autocrine activities of basic fibroblast growth factor: regulation of endothelial cell movement, plasminogen activator synthesis and DNA synthesis. *J. Cell Biol.* **1988**, *107*, 1199–1205.

(16) Toffoli, S; Roegiers, A; Feron, O; Steenbrugge, M. V.; Ninane, N.; Raes, M.; Michiels, C. Intermittent hypoxia is an angiogenic inducer for endothelial cells: role of HIF-1. *Angiogenesis* **2009**, *12*, 47–67.

(17) Ishikawa, H.; Heaney, A. P.; Yu, R.; Horwitz, G. A.; Melmed, S. Human pituitary tumor-transforming gene induces angiogenesis. *J. Clin. Endocrinol. Metab.* **2001**, *86*, 867–874.

(18) Denekamp, J. Angiogenesis, neovascular proliferation and vascular pathophysiology as targets for cancer therapy. *Br. J. Radiol.* **1993**, *66*, 181–196.